Synthesis and characterization of ZnS:Mn/ZnS core/shell nanoparticles for tumor targeting and imaging invivo

Article *in* Journal of Biomaterials Applications · April 2012

DOI: 10.1177/0885328212444642 · Source: PubMed

5 authors, including:

Yu Zhangsen
Shaoxing University
11 PUBLICATIONS **59** CITATIONS

Journal of Biomaterials Applications
http://jba.sagepub.com/

Synthesis and characterization of ZnS: Mn/ZnS core/shell nanoparticles for tumor targeting and imaging in vivo

Zhangsen Yu, Xiying Ma, Bin Yu, Yuefang Pan and Zhaogang Liu

J Biomater Appl published online 24 April 2012
DOI: 10.1177/0885328212444642

The online version of this article can be found at:
http://jba.sagepub.com/content/early/2012/04/05/0885328212444642

Published by:
SAGE
http://www.sagepublications.com

Article

JOURNAL OF
biomaterials
applications

Journal of Biomaterials Applications
0(0) 1–9

DOI: 10.1177/0885328212444642
jba.sagepub.com
SAGE

Synthesis and characterization of ZnS:Mn/ZnS core/shell nanoparticles for tumor targeting and imaging in vivo

Zhangsen Yu[1], Xiying Ma[2], Bin Yu[1], Yuefang Pan[1] and Zhaogang Liu[1]

Abstract

Fluorescence imaging technique has been used for imaging of biological cells and tissues in vivo. The Cd-free luminescent quantum dots conjugating with a cancer targeting ligand has been taken as a promising biocompatibility and low cytotoxicity system for targeted cancer imaging. This work reports the synthesis of fluorescent-doped core/shell quantum dots of water-soluble manganese-doped zinc sulfide. Quantum dots of manganese-doped zinc sulfide were prepared by nucleation doping strategy, with 3-mercaptopropionic acid as stabilizer at 90°C in aqueous solution. The manganese-doped zinc sulfide nanoparticles exhibit strong orange fluorescence under UV irradiation, resistance to photo-bleaching, and low-cytotoxicity to HeLa cells. The structure and optical properties of nanoparticles were characterized by scanning electron microscope, X-ray diffraction, dynamic light scattering, and photoluminescence emission spectroscopy. Manganese-doped zinc sulfide nanoparticles conjugated with folic acid using 2,2′-(ethylenedioxy)-bis-(ethylamine) as the linker. The covalent binding of both 2,2′-(ethylenedioxy)-bis-(ethylamine) and folic acid on the surface of manganese-doped zinc sulfide nanoparticles probed by Fourier transform infrared spectroscopy detection. Furthermore, in vitro cytotoxicity assessment of manganese-doped zinc sulfide–folic acid probes use HeLa cells. The obtained fluorescent probes (manganese-doped zinc sulfide) were used for tumor targeting and imaging in vivo. The manganese-doped zinc sulfide–folic acid fluorescent probes which targeting the tumor cells in the body of nude mouse tumor model would emit orange fluorescence, when exposed to a 365 nm lamp. We investigate the biodistribution of the manganese-doped zinc sulfide–folic acid fluorescent probes in tumor mouse model by measuring zinc concentration in tissues. These studies demonstrate the practicality of manganese-doped zinc sulfide–folic acid fluorescent probes as promising platform for tumor targeting and imaging in vivo.

Keywords

ZnS:Mn/ZnS nanoparticles, fluorescence, tumor targeting and imaging, in vivo, cytotoxicity

Introduction

Quantum dots (QDs) possess unique optical properties that make them potential candidates as fluorescent probes for tumor targeting and imaging in vivo.[1–5] They have narrow, symmetrical, and tunable emission profiles, broad excitation band and large Stokes shift, high luminescence quantum yields, and excellent photochemical stability.[6] Recently, QDs have been widely used in biomedical fields due to their unique properties.[7–10]

To date, the most excellent photoluminescence QDs have been synthesized through many methods and used in biomedical fields. Unfortunately, most QDs contain high toxic elements, such as cadmium, tellurium, and mercury, which are toxic and fatal to biological system.[11–13] The cytotoxicity of QDs is the major drawback that severely limits the use of QDs in biomedical applications. Most of the current QDs probes are based on CdS, CdSe, PbSe, and CdSe/ZnS, so they cannot be used for any human clinical applications because of their cytotoxicity. This cytotoxicity results mainly

[1]School of Medicine, Shaoxing University, Shaoxing, P. R. China
[2]School of Mathematics and Physics, Suzhou University of Science and Technology, Jiangsu, P. R. China

Corresponding author:
Zhangsen Yu, School of Medicine, Shaoxing University, Shaoxing 312000, P. R. China
Email: yzs@usx.edu.cn

from the decomposition and release of heavy metal ions and the formation of high-reactive oxygen species.[14–16] Therefore, in recent articles, the Cd-free ZnS-based QDs are extremely promising candidates for biomedical applications.[17–19]

Considering the above, it is very important to develop low cytotoxicity quantum dots with essential attributes, such as, water solubility, biocompatibility, high luminescence, and photo stability. In recent years, many groups have focused their attention on ZnS and doped ZnS (such as ZnS:Mn, ZnS:Cu) QDs.[20–23] And the ZnS-based nanoparticles have a wide range of applications in the quantitative analysis of ions and molecules, immunoassays to live cells and tumor cells imaging in vitro. In order to improve quantum yields, the ZnS shell was subsequently over-coated around the ZnS:Mn or ZnS:Cu core nanoparticles.[24]

In this study, we have developed a facile strategy for the synthesis of water-soluble manganese-doped zinc sulfide (ZnS:Mn/ZnS) core/shell quantum dots stabilized with 3-mercaptopropionic acid (MPA). These QDs are uniform in size, stable in water, and easy for conjugation after surface modification with MPA. In order to achieve targeting and fluorescence imaging tumor in vivo, the ZnS:Mn/ZnS QDs functionalized with folic acid (FA) using 2,2′-(ethylenedioxy)-bis-(ethylamine) (EDBE) as the linker in the presence of N-hydroxysuccinimide (NHS) and 1-ethyl-3-(3-dimethylaminopropyl) carbodiimide hydrochloride (EDC). Cytotoxicity study was carried out using ZnS:Mn/ZnS-FA probes on HeLa cells. The FA-modified probes determine the folate receptors (FRs) which served as a target for fluorescence imaging, because the FRs express with high binding affinity for FA in several cancers (such as cervical, breast, lung, and colorectal cancers).[25] Furthermore, the FR is only minimally distributed in normal tissues. We explore the use of the ZnS:Mn/ZnS-FA fluorescent probes for tumor targeting and imaging in vivo.

Experiment

Materials

Analytical reagents $Zn(CH_3COO)_2{\cdot}2H_2O$, $Mn(CH_3COO)_2{\cdot}4H_2O$, $Na_2S{\cdot}9H_2O$, NaOH, anhydrous ethanol, and 3-mercaptopropionic acid (MPA) were purchased from Sinopharm Chemical Reagent Co., Ltd. and used as received. FA, N-hydroxysuccinimide (NHS), 1-ethyl-3-(3-dimethylaminopropyl) carbodiimide hydrochloride (EDC), and 2,2′-(ethylenedioxy)-bis-(ethylamine) (EDBE) were obtained from Aldrich and used as received. Deionized water with a resistivity of 18.25MΩ·cm was employed in the experiments.

Synthesis of water-soluble ZnS:Mn/ZnS nanoparticles by nucleation doping strategy

This study reports a facile aqueous nucleation doping route to synthesize water-soluble ZnS:Mn/ZnS nanoparticles. All solutions were prepared at room temperature. The stock solutions were prepared by adding appropriate amount of $Zn(CH_3COO)_2{\cdot}2H_2O$ and $Mn(CH_3COO)_2{\cdot}4H_2O$ into 100 mL of MPA aqueous solution, respectively. The pH of the mixed solutions was adjusted to 4.5 by 4.0 M NaOH solution. Then the Mn-MPA stock solution was added into the Na_2S solution drop by drop under vigorous stirring in the three-necked flask. The reaction solution was stirred at 90°C for 20 min to form small-sized MnS core. In order to obtain ZnS:Mn/ZnS core/shell nanoparticles with ZnS shell, the Zn-MPA aqueous solution was quickly added into the Na_2S solution at two steps. At the first step, 70% of Zn-MPA stock solution was quickly added into Na_2S solution with vigorously stirring, reacting for 30 min with stirring, and aging for 20 h at the same temperature. At the second step, residual Zn-MPA stock solution was injected and heated at 90°C for another 4 h. The argon gas was bubbling for the whole reaction process in order to remove oxygen. Finally, the reaction was cooled to room temperature, and the nanoparticles were precipitated with anhydrous ethanol. And then the precipitation was centrifuged, washed with anhydrous ethanol several times, and dried in vacuum.

Coupling of ZnS:Mn/ZnS nanoparticles with FA

QDs-FA conjugates were obtained using EDC in the presence of NHS. In the experiment, the water-soluble ZnS:Mn/ZnS nanoparticles (0.25 mg) were dispersed in 10 mL of phosphate-buffered saline (PBS). To 10 mL of ZnS:Mn/ZnS, 50μL of EDBE (0.15 M in PBS, pH 7.4), EDC (0.15 M in PBS, pH 7.4), and an equal amount of NHS (0.30 M in PBS, pH 7.4) were added and stirred for 40 min at 37°C. And then, nanoparticles were recovered by precipitation with anhydrous ethanol, washed several times with anhydrous ethanol, and dried under vacuum. Finally, the EDBE-modified ZnS:Mn/ZnS nanoparticles (0.5 mg) was dispersed in 10 mL of PBS. In all, 50 μL of EDC (0.30 M in PBS, pH 7.4), NHS (0.60 M in PBS, pH 7.4), and an equal amount of FA (0.30 M in PBS, pH 7.4) was added. The reaction incubated at 37°C for 12 h. The FA-labeled ZnS:Mn/ZnS nanoparticles (ZnS:Mn/ZnS-FA) were purified using 4.0 kDa molecular weight dialysis kit for 20 h and washed several times with PBS. The QDs-FA were dispersed into PBS solution and stored in dark at room temperature.

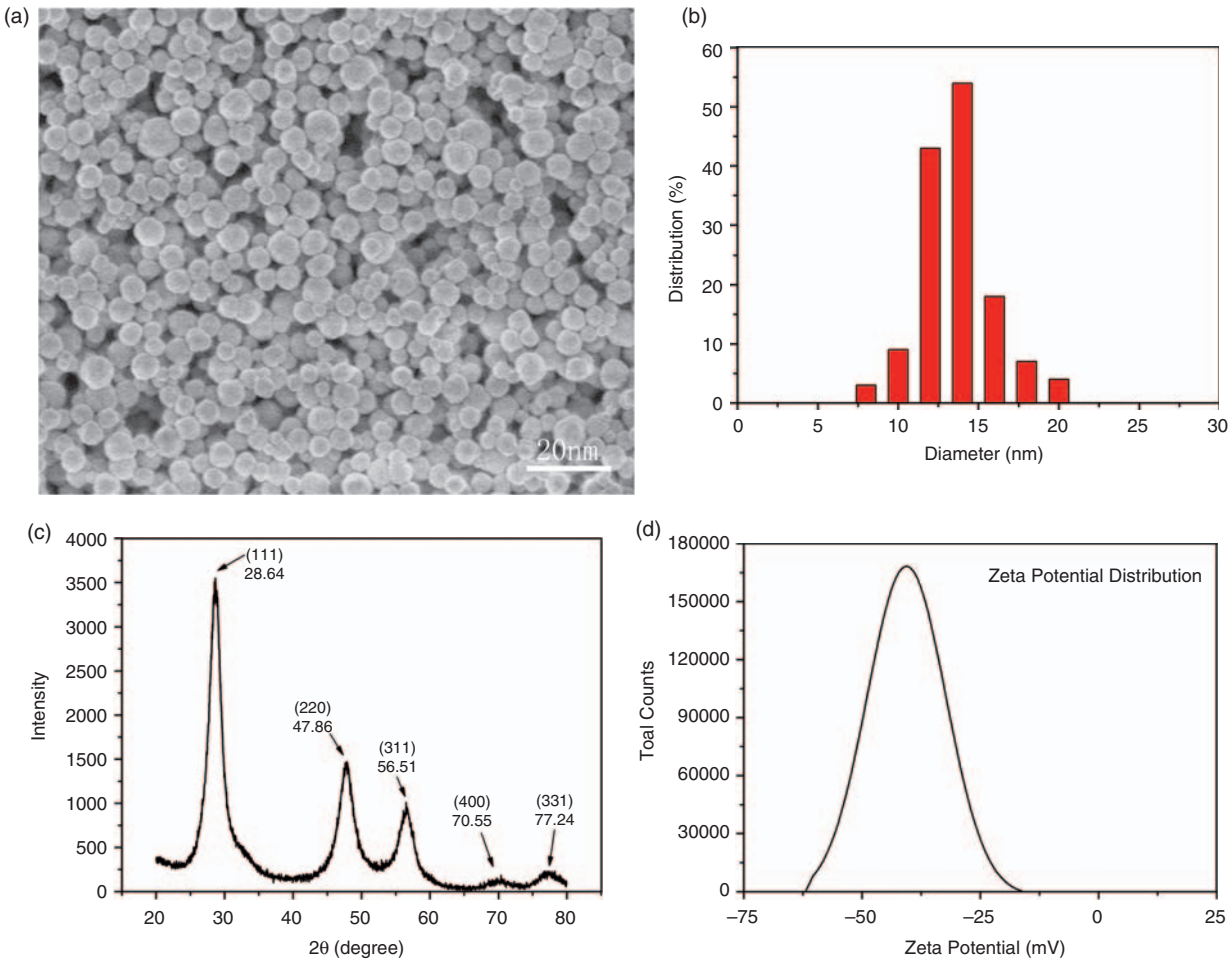

Figure 1. Scanning electron microscope (SEM) image (a), diameter distribution (b), X-ray diffraction (XRD) pattern (c), and zeta potential distribution (d) of the manganese-doped zinc sulfide (ZnS:Mn/ZnS) quantum dots (QDs).

Cell viability test

HeLa cells were used to assess the cell viability of the ZnS:Mn/ZnS-FA probes. The cells were seeded into a 96-well cell culture plate at a density of 5×10^3/well. After 24 h of culture, different concentrations of ZnS:Mn/ZnS-FA probes were then added to the wells. The cells were subsequently incubated at various time points (6 h or 24 h) and then the MTT solution (20 μL, 5.0 mg/mL in PBS, Ph 7.4) was added to each well. The cells were incubated for an additional 3 h at 37°C. After removing the medium, the 100 μL dimethyl sulfoxide (DMSO) was added into each well to completely dissolve the MTT crystals. And the absorbance intensity of the cell lysate at 570 nm of each well was measured with a multifunction microplate reader (TECAN). The quantity of the formazan product formed as measured by the amount of 570 nm absorbance is directly proportional to the number of living cells in the culture. The relative cell viability related to control wells containing cell culture medium without nanoparticles was calculated by: cell viability (%) = (mean of Abs. value of treatment group/mean of Abs. value of control) × 100%.

Fluorescence microscope imaging of HeLa cells

The HeLa cells were cultured in flasks in a medium made up of DMEM, antibiotics, and foetal bovine serum (FBS), and incubated in a 100% humidified incubator with 5% CO_2 at 37°C. The cells were plated on 14-mm glass coverslips and allowed to adhere for 24 h. Subsequently, ZnS:Mn/ZnS-FA probes (100 μL, 5.0 mg/mL) were added and the HeLa cells were incubated for 4 h at 37°C under CO_2 5%, and then washed with phosphate buffer solution (PBS) 3 to 5 times to remove excess probes. In order to prove that the ZnS:Mn/ZnS-FA probes label HeLa cells via interaction with FA receptors present at the surface of the cells, we conducted competition experiments while the ZnS:Mn/ZnS nanoparticles and HeLa cells were incubated under the same experimental conditions. And

then, the ZnS:Mn/ZnS-FA probes and ZnS:Mn/ZnS nanoparticles labelled HeLa cells were imaged in bright field and under exposure to 365 nm ultraviolet excitation using a Nikon fluorescence microscope (ECLIPSE 80i), respectively.

Fluorescence imaging and biodistribution in vivo

The prepared ZnS:Mn/ZnS-FA were used as the fluorescent probes. The tumor mouse model was established by subcutaneous injection of 7×10^5 HeLa cells in PBS into the back of 5- to 7-week-old female BALB/C nude mouse. Tumor growth was observed daily until it reached a size of ~0.5 cm in diameter. ZnS:Mn/ZnS-FA (100 μL, 5.0 mg/mL) was injected into the tail vein. The nude mouse was anesthetized by injection of a ketamine at a dosage of 100 mg/kg. In a dark room, the nude mouse was set under irradiation with 365 nm UV lamp. Fluorescent images were recorded by using an ordinary digital camera (SONY, DSC-T70) after the injected ZnS:Mn/ZnS-FA adequately penetrated into the tumor (about 10 min post-injection). After fluorescent imaging, the mice were killed by overdose of CO_2. Tumor, blood, and major organs, such as lung, heart, liver, spleen, and kidney, were removed for biodistribution studies. The biodistribution of ZnS:Mn/ZnS nanoparticles was based on the measurement of zinc concentration in the blood and major organs by using inductively coupled plasma atomic emission spectroscopy (ICP-AES, Leeman, Prodigy xp). Briefly, the nude mice were euthanized at 15 min and 24 h. The major organs, tumor, and blood were collected, weighted, and incubated at 37°C overnight in digestion buffer solution. The digested samples were diluted 20 times before the ICP-AES analysis. Zinc contents in the samples were then determined by ICP-AES as a means of determining ZnS:Mn/ZnS-FA probes concentration.

Results and discussion

Synthesis and characterization of ZnS:Mn/ZnS nanoparticles

The prepared ZnS:Mn/ZnS nanoparticles were characterized by scanning electron microscope (SEM, JSM-6360LV), X-ray diffraction (XRD, PANalytical's X'Pert PRO) and zeta potential measurements (Zetasizer NanoZS, Malvern Inst., Malvern, UK). The optical characteristics of ZnS:Mn/ZnS were examined by UV/Vis spectrophotometer (Beckman Coulter DU 800) and spectrofluorimeter (F-7000, Hitachi, Tokyo, Japan).

MPA-coated ZnS:Mn/ZnS nanoparticles were synthesized by nucleation doping strategy as previously reported, with modification.[26] The ZnS:Mn/ZnS nanoparticles were hydrophilic and could disperse well in water. The SEM image of the ZnS:Mn/ZnS nanoparticles is shown in Figure 1(a). The ZnS:Mn/ZnS nanoparticles are well-dispersed spherical nanoparticles and

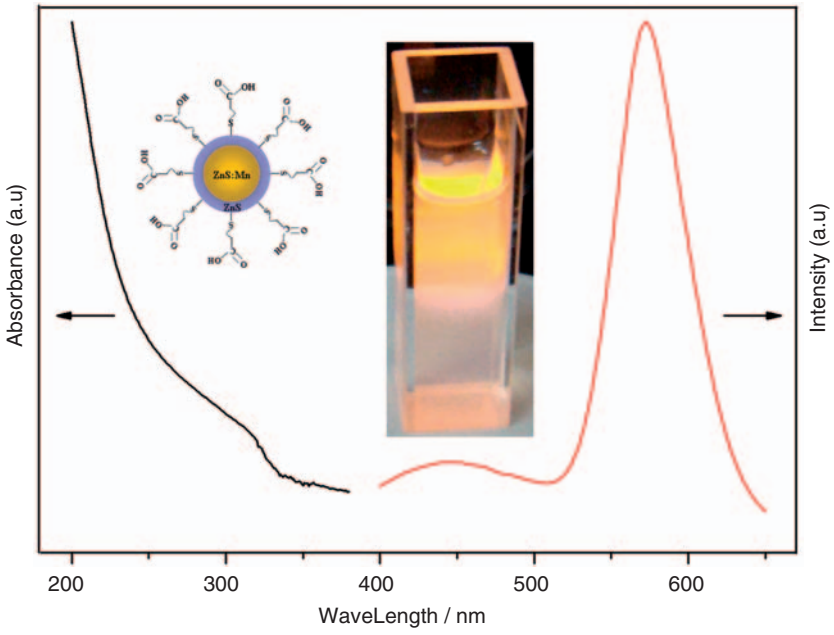

Figure 2. Photoluminescence emission spectrum and absorption spectrum of the water-soluble manganese-doped zinc sulfide (ZnS:Mn/ZnS) quantum dots (QDs) in aqueous solution. Two inserted images refer to the schematically of ZnS:Mn/ZnS QDs, and the QDs solution under a UV lamp irradiation with the wavelength of 365 nm, respectively.

uniform in size with a mean diameter of about 8.0 nm. The hydrodynamic diameter and size distribution of ZnS:Mn/ZnS nanoparticles were determined by dynamic light scattering (DLS) (Figure 1(b)). The zeta potential of the ZnS:Mn/ZnS nanoparticles also determined by DLS was estimated to be −40.6 mV, and Figure 1(d) shows the Zeta potential distribution.

The crystalline structures of nanoparticles were determined by XRD. The XRD pattern of the ZnS:Mn/ZnS nanoparticles is shown in Figure 1(c). These diffraction features appearing at 28.6°,47.9°, 56.5°, 70.6°, and 77.2° corresponded to the (111), (220), (311), (400), and (331) planes of cubic zinc blende structure, which matches well with the standard card (JCPDS NO. 05-0566). The diffraction peaks are greatly broadened in comparison with those of bulk ZnS, which was characteristic of nanocrystal particle. In addition, no feature peaks of impurity phases are observed in the XRD pattern, indicating the high purity of the ultimate products. From this diffractogram, the crystalline sizes of the ZnS:Mn/ZnS nanoparticles can be calculated by Scherrer's equation. According to the full width at half maximum of (111) zinc blende reflection, the estimated average size is 5.4 nm.

Figure 2 contains the absorption and emission spectra of ZnS:Mn/ZnS nanoparticles in aqueous solutions. The core/shell ZnS:Mn/ZnS nanoparticles exhibit a strong yellow peak (575 nm) which is ascribed to the energy transition from $^4T_1$ excited state to the $^6A_1$ ground state of the Mn^{2+} ion within a nanocrystalline ZnS lattice. In addition, the weak intensity broad emission centered at ~450 nm, presumably due to surface trap emission of the ZnS. The ZnS:Mn/ZnS nanoparticles demonstrate an absorption feature at 310 nm. On the basis of the UV absorption spectrum, the sizes of these ZnS:Mn/ZnS nanoparticles are between 5.0 nm and 10.0 nm. This is in excellent agreement with the SEM, XRD, and DLS reported above. In addition, the quantum yield (QY) was determined relative to Rhodamine 6G in water (QY = 95%). And the photoluminescence QY of ZnS:Mn/ZnS nanoparticles is about 18.6%. After the ZnS:Mn/ZnS nanoparticles were conjugated with EDBA and FA, the ZnS:Mn/ZnS-EDBE (16.1%) and ZnS:Mn/ZnS-EDBE-FA (13.6%) showed a decrease in QY.

Figure 3 shows the ZnS:Mn/ZnS nanoparticles were continually exposed to a 365-nm UV lamp and the emission intensity was recorded during 5 h with no reduction in emission intensity. The ZnS:Mn/ZnS nanoparticles show an increased photoluminescence intensity during the first 50 min of exposure time, and

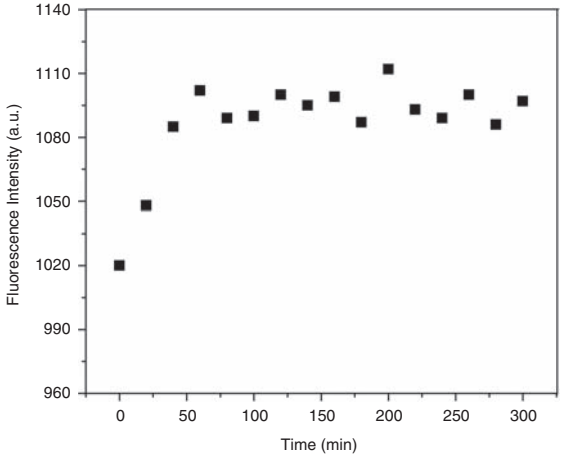

Figure 3. Dried manganese-doped zinc sulfide (ZnS:Mn/ZnS) nanoparticles continually exposed to 365 nm lamp as a function of exposure time.

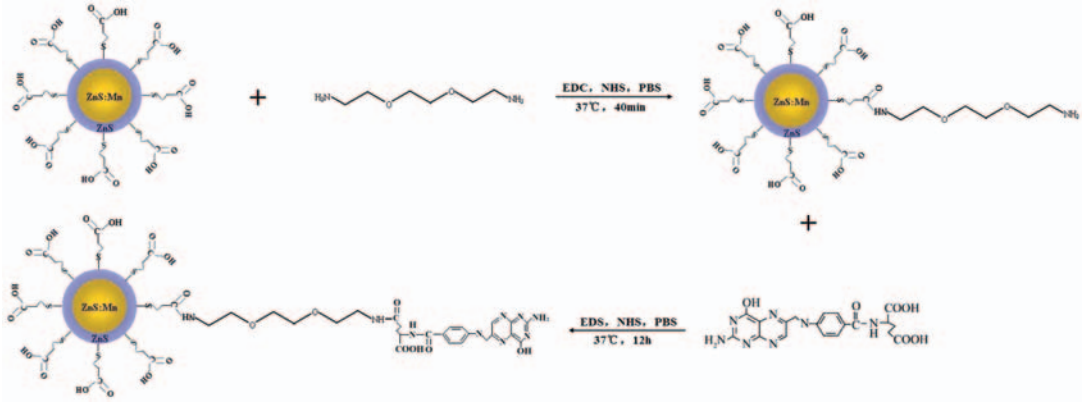

Figure 4. Schematic illustration of the synthetic manganese-doped zinc sulfide (ZnS:Mn/ZnS)-folic acid (FA) probes conjugate using a 2,2′-(ethylenedioxy)-bis-(ethylamine) (EDBE) linker in the presence of 1-ethyl-3-(3-dimethylaminopropyl) carbodiimide hydrochloride (EDC) and N-hydroxysuccinimide (NHS).

then demonstrated strong resistance to photo-bleaching. This is because a passivating surface formed as a result of photo-oxidation and was responsible for the high increase of the photoluminescence emission upon irradiation.[27]

In order to improve fluorescence properties of the ZnS:Mn/ZnS nanoparticles, the previous report has discussed the influence of the synthesis conditions such as different Mn^{2+} concentrations, different ratios of the MPA/Zn, and different thicknesses of the ZnS shell, on the luminescent properties of ZnS:Mn/ZnS QDs.[24]

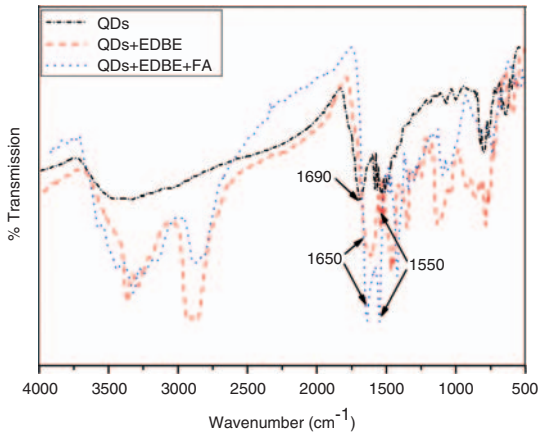

Figure 5. Fourier transform infrared spectroscopy (FTIR) spectra of manganese-doped zinc sulfide (ZnS:Mn/ZnS) nanoparticles, ZnS:Mn/ZnS-2,2′-(ethylenedioxy)-bis-(ethylamine) (EDBE) and ZnS:Mn/ZnS-EDBE-folic acid (FA).

Synthesis of ZnS:Mn/ZnS-FA probes and FTIR study

The cross-linking of FA to the surface of ZnS:Mn/ZnS nanoparticles was realized by EDBE as a linker. One of the two amine groups of EDBE first reacted with an carboxyl group present on the surface of the ZnS:Mn/ZnS nanoparticles. And then, the amine groups on the surface of ZnS:Mn/ZnS nanoparticles reacted with the γ carboxyl of FA. This reaction was achieved in the presence of EDC and NHS. Figure 4 shows the typical synthetic procedure of ZnS:Mn/ZnS-FA probes.

In order to show the formation of amide bonds among ZnS:Mn/ZnS nanoparticles, EDBE and FA, the conjugation of FA onto the ZnS:Mn/ZnS nanoparticles was confirmed from Fourier transform infrared spectroscopy (FTIR, Hermo-Nicolet Nexus 670). The comparison of FTIR spectra of the ZnS:Mn/ZnS, ZnS:Mn/ZnS-EDBE and ZnS:Mn/ZnS-EDBE-FA is shown in Figure 5. The basic characteristic FTIR band of ZnS:Mn/ZnS nanoparticles is displayed at 1690 cm^{-1} (−COOH). ZnS:Mn/ZnS-EDBE shows the characteristic absorption bands at 1650 cm^{-1} (amide I) and 1550 cm^{-1} (amide II). The presence of these two bands indicates that an amide bond has been formed between the −COOH of ZnS:Mn/ZnS nanoparticles and the $-NH_2$ amine end group of EDBE. And the

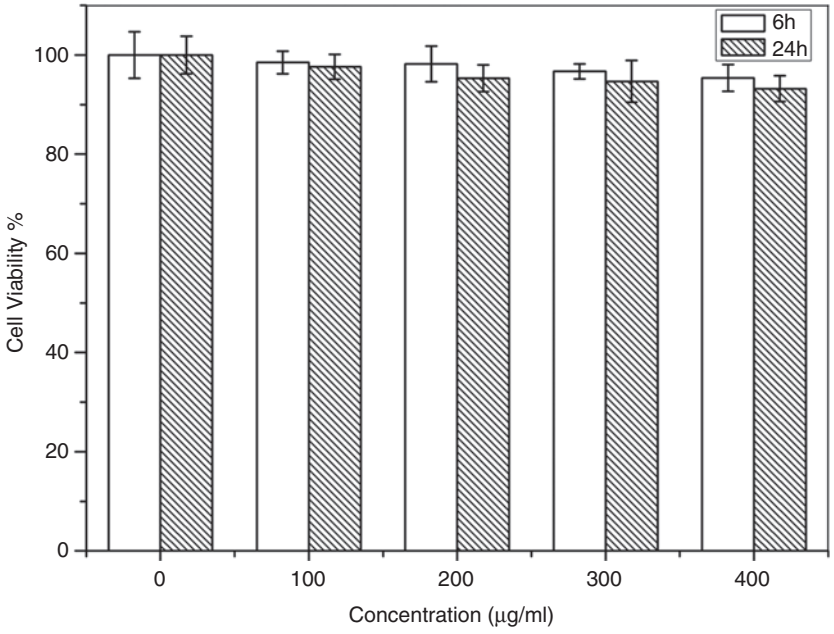

Figure 6. Cytotoxicity of manganese-doped zinc sulfide (ZnS:Mn/ZnS)-folic acid (FA) probes toward HeLa cells for 6 or 24 hours at 37°C measured by MTT assay.

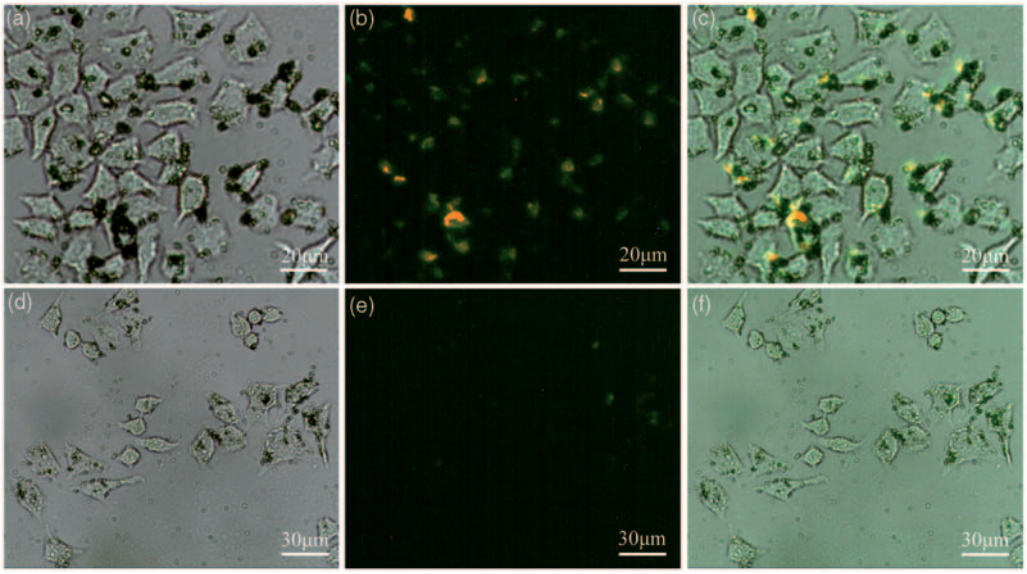

Figure 7. Fluorescent microscopic images showing interaction of manganese-doped zinc sulfide (ZnS:Mn/ZnS)-folic acid (FA) probes (a-c) and ZnS:Mn/ZnS nanoparticles (d-f) with HeLa cells. The left figure correspond to transmission image, fluorescence image is shown in the middle, and the right figure show overlays of the transmission and fluorescence imaging. The images were obtained with laser excitation at 365 nm.

same two bands have become more intense in ZnS:Mn/ZnS−EDBE-FA. This proves the formation of an extra amide bond after coupling of FA.

MTT cell viability assay

Figure 6 shows the toxicity effects of varying concentrations from 0 to 400 μg/mL of ZnS:Mn/ZnS-FA probes on HeLa cell viability using an MTT assay. The HeLa cells were cultured for 6 h or 24 h in medium containing ZnS:Mn/ZnS-FA probes. All MTT assays demonstrated that the cell viability decreased with the increasing QDs concentration. After 6 h of incubation with ZnS:Mn/ZnS-FA probes, the cell viabilities were greater than 95%. It can be seen that the probes show 93% cell viability, which is maintained even up to high dose of 400 μg/mL and 24 h of incubation. The cell viability still remains at ~90% for the ZnS:Mn/ZnS-FA probes at various concentrations. The MTT assay results demonstrated that the obtained ZnS:Mn/ZnS-FA probes could be a better alternative to organic fluorescent probes for imaging in vivo due to their low cytotoxicity nature.

Interaction of HeLa cell with ZnS:Mn/ZnS-FA QDs

FA-coated ZnS:Mn/ZnS nanoparticles were incubated in an appropriate culture medium with HeLa cells. The HeLa cells are known to express high levels of FRs on the cell surface. And FA can specifically target FRs. After 4 h, the HeLa cells were washed and imaged in bright field (Figure 7(a)) and under exposure to 365 nm ultraviolet radiation using a Nikon fluorescence microscope. Figure 7(b) shows the intense intracellular fluorescence. The overlays of the transmission and

Figure 8. In vivo targeting and imaging of a HeLa tumor cells in nude mouse using a manganese-doped zinc sulfide (ZnS:Mn/ZnS)-folic acid (FA) conjugate.

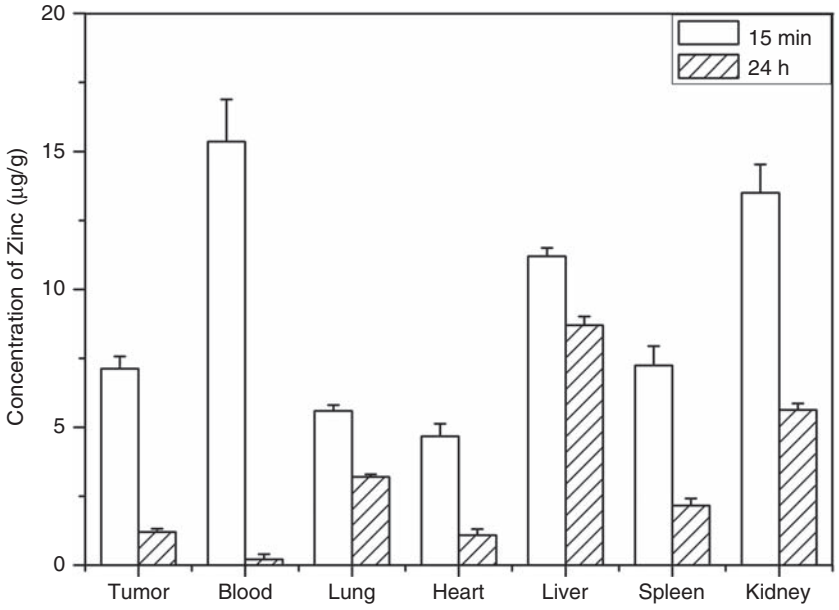

Figure 9. Biodistribution of manganese-doped zinc sulfide (ZnS:Mn/ZnS)-folic acid (FA) probes in organs of nude mouse harvested after tail-vein injection.

fluorescence image (Figure 7(c)) proved that fluorescence was correlated with the intracellular region. Moreover, weak nanoparticles uptake (Figure 7(d)) and no fluorescence sign (Figure 7(e)) to the HeLa cells were observed upon after the incubation with the ZnS:Mn/ZnS nanoparticles in the competition experiment. In these conditions, HeLa cells do not uptake the free FA ZnS:Mn/ZnS nanoparticles. This result provides evidence for the targeting specificity of FA-linked ZnS:Mn/ZnS nanoparticles to FR of HeLa cells.

Tumor targeting, imaging, and biodistribution in vivo

Figure 8 shows fluorescence imaging result obtained from ZnS:Mn/ZnS-FA probes injected into the tail vein of a nude mouse tumor model. The image clearly shows the tumor tissue exhibits strong orange fluorescence. In contrast, the whole nude mouse shows weak reflected light background. These results indicate that the ZnS:Mn/ZnS-FA probes have high binding affinity to HeLa cells in vivo and are sensitive enough for location analysis of the tumor in vivo. In addition to the tumor imaging investigation, we have studied the biodistribution of ZnS:Mn/ZnS-FA probes in vivo. Figure 9 shows the zinc concentration in major organs, blood, and tumor. We have found that the uptake of ZnS:Mn/ZnS-FA probes mainly occurred in the liver, kidney, lung, and spleen, with little probes accumulation in the tumor, heart, and blood.

Conclusion

In conclusion, a simple method was used to synthesize heavy metal free ZnS:Mn/ZnS core/shell nanoparticles. The nanoparticles have spherical shape and the average size of about 8.0 nm in diameter and show strong yellow fluorescence in aqueous solutions when excited at 365 nm lamp. Moreover, we report the biocompatibility, cytotoxicity, tissue distribution, and application of ZnS:Mn/ZnS-FA fluorescence probes for in vivo tumor imaging. To the best of our knowledge, this represents the first report of tumor targeting and imaging in vivo of ZnS:Mn/ZnS nanoparticles in nude mouse.

Funding

This work was supported in parts by the National Natural Science Foundation of China (No. 60976071) and a scientific project of Shaoxing University (2011LG1018).

References

1. Chan WCW and Nie SM. Quantum dot bioconjugates for ultrasensitive nonisotopic detection. *Science* 1998; 281: 2016–2018.
2. Bruchez M, Moronne M, Gin P, et al. Semiconductor nanocrystals as fluorescent biological labels. *Science* 1998; 281: 2013–2016.
3. Gao XH, Cui YY, Richard ML, et al. In vivo cancer targeting and imaging with semiconductor quantum dots. *Nat Biotechnol* 2004; 22: 969–976.

4. Liang DC, Liu J, Yu XF, et al. Biocompatibility of quantum dot probes used for targeted imaging of hepatocellular carcinoma metastasis. *Biomaterials* 2008; 29: 4170–4176.
5. Nobuyuki K, Thomas EM, Makoto M, et al. Real-time optical imaging using quantum dot and related nanocrystals. *Nanomed* 2010; 5: 765–776.
6. Suyver JF, Wuister SF, Kelly JJ, et al. Synthesis and photoluminescence of nanocrystalline ZnS:Mn^{2+}. *Nano Lett* 2001; 1: 429–433.
7. Wang L and Fu J. One-step aqueous synthesis of CdS nanoparticles as a novel fluorescence probe for the ultrasensitive detection of DNA. *J Lumines* 2010; 130: 845–850.
8. Hoshino A, Hanada S, Manabe N, et al. Immune response induced by fluorescent nanocrystal quantum dots in vitro and in vivo. IEEE Trans. *Nanobioscience* 2009; 8: 51–57.
9. Sarwat BR, Shirin G, Keshtgar M, et al. Semiconductor quantum dots as fluorescent probes for in vitro and in vivo bio-molecular and cellular imaging. *Nano Rev* 2010; 1: 5161–5165.
10. Laurent AB, Yuval E and Weiss S. Quantum dots for in vivo small-animal imaging. *J Nucl Med* 2009; 50: 493–496.
11. Nel A, Xia T, Madler L, et al. Toxic potential of materials at the nanolevel. *Science* 2006; 311: 622–627.
12. Walther UI, Walther SC and Temruck O. Effect of enlarged glutathione on zinc-mediated toxicity in lung-derived cell lines. *Toxicol Vitro* 2007; 21: 380–386.
13. Klaine SJ, Alvarez PJJ, Batley GE, et al. Nanomaterials in the environment: behavior, fate, bioavailability and effects. *Environ Toxicol Chem* 2008; 27: 1825–1851.
14. Kirchner C, Liedl T, Kudera S, et al. Cytotoxicity of colloidal CdSe and CdSe/ZnS nanoparticles. *Nano Lett* 2005; 5: 331–338.
15. Schneider R, Wolpert C, Guilloteau H, et al. The exposure of bacteria to CdTe-core quantum dots: the importance of surface chemistry on cytotoxicity. *Nanotechnology* 2009; 20: 225101.
16. Zhang Y, He J, Wang PN, et al. Time-dependent photoluminescence blue shift of the quantum dots in living cells: effect of oxidation by singlet oxygen. *J Am Chem Soc* 2006; 128: 13396–13401.
17. He Y, Wang HF and Yan XP. Exploring Mn-doped ZnS quantum dots for the room-temperature phosphorescence detection of enoxacin in biological fluids. *Anal Chem* 2008; 80: 3832–3837.
18. Manzoor K, Johny S, Thomas D, et al. Bio-conjugated luminescent quantum dots of doped ZnS: a cyto-friendly system for targeted cancer imaging. *Nanotechnology* 2009; 20: 065102.
19. Geszke M, Murias M, Balan L, et al. Folic acid-conjugated core/shell ZnS:Mn/ZnS quantum dots as targeted probes for two photon fluorescence imaging of cancer cells. *Acta Biomater* 2011; 7: 1327–1338.
20. Bhargava RN, Gallagher D, Hong X, et al. Optical properties of manganese doped nanocrystals of ZnS. *Phys Rev Lett* 1994; 72: 416–419.
21. Chung JH, Ah CS and Jang DJ. Formation and distinctive decay times of surface- and lattice- bound Mn^{2+} impurity luminescence in ZnS nanoparticles. *J Phys Chem B* 2001; 105: 4128–4132.
22. Cao LX, Zhang JH and Ren SH. Luminescence enhancement of core-shell ZnS:Mn/ZnS nanoparticles. *Appl Phys Lett* 2002; 80: 4300–4302.
23. Chien ND, Chung HV, Huy PT, et al. Mn, Cu doping and optical properties of highly crystalline ultralong ZnS nanowires. *Adv Mater Res* 2008; 31: 114–116.
24. Yu ZS and Ma XY. Synthesis and photoluminescence of water-soluble ZnS:Mn^{2+}/ZnS quantum dots by nucleation doping strategy. *Nano* 2011; 6: 75–79.
25. Ross JF, Chaudhuri PK and Ratnam M. Differential regulation of folate receptor isoforms in normal and malignant tissues in vivo and in established cell lines. *Cancer* 1994; 73: 2432–2443.
26. Fang Z, Wu P, Zhong XH, et al. Synthesis of highly luminescent Mn:ZnSe/ZnS nanocrystals in aqueous media. *Nanotechnology* 2010; 21: 305604.
27. Ageeth AB and Andries M. Luminescence quantum efficiency of nanocrystalline ZnS:Mn^{2+}. 2. Enhancement by UV irradiation. *J Phys Chem B* 2001; 105: 10203–10209.